

# Metallurgical examination of rockbolts failed in service due to stress corrosion cracking

**E. Elias** *University of New South Wales, Australia*

**D. Vandermaat** *University of New South Wales, Australia*

**P. Craig** *Jennmar Australia Pty Ltd, and University of New South Wales, Australia*

**H. Chen** *University of New South Wales, Australia*

**A. Crosky** *University of New South Wales, Australia*

**S. Saydam** *University of New South Wales, Australia*

**P. Hagan** *University of New South Wales, Australia*

**B. Hebblewhite** *University of New South Wales, Australia*

## Abstract

*In recent years, increasingly higher strength grades of steel have been used to meet the increasingly demanding requirements placed on rockbolts in underground coal mines. An unfortunate consequence of this has been the occurrence of premature failure of the rockbolts due to stress corrosion cracking. Stress corrosion cracking is a complex phenomenon which involves slow, progressive crack growth under the application of a sustained load (either residual or applied) in what is usually only a mildly corrosive environment. The failure occurs in a brittle manner below the ultimate tensile strength of the material.*

*An understanding of the mechanisms associated with rockbolt failure is imperative in order to develop effective strategies that will reduce the incidence of failure. This paper reports on a forensic investigation directed towards this goal. The work involved fractographic analysis of failed rockbolts retrieved from underground coal mines, identification of the corrosion product in the stress corrosion cracks, and analysis of mine water from affected areas in the mines. It was found that two distinctly different types of mine water were associated with the stress corrosion cracking failures, these being high pH and near neutral pH. The fractographic analysis showed that the micro-mechanism of stress corrosion cracking was quite different for the two types of minewater. Different types of corrosion product were observed within the stress corrosion cracks produced from each of the two different minewaters, providing further confirmation that the stress corrosion cracking mechanism was different in the two cases.*

## 1 Introduction

Underground coal mines rely extensively on effective ground control through the use of resin-grouted rockbolts. These were first used in the Australian underground coal industry in the 1940s at the Elrington Colliery in NSW that was owned and operated by BHP Billiton (Gardener, 1971). Nowadays rockbolts have been implemented in the underground mining, civil engineering and tunnelling industries. Rockbolts have now become a major part in the Australian mining industry by having the ability to improve underground roof conditions as well as the productivity and efficiency of underground mining. However, any failure of rockbolts drastically decreases the stability of the roof which has serious implications for both the mine operations and personnel safety.

Nevertheless, rockbolts are considered reliable enough to be used in harsh environments where there are problematic ground conditions such as high stress levels and the presence of corrosive groundwater. Characteristically, when a failed rockbolt from this environment is examined, there is a discoloured region at the fracture origin which is characteristic of stress corrosion cracking (SCC) (Crosky et al., 2012, 2004,

2002). SCC is defined as slow, progressive crack growth under the application of a sustained load (either residual or applied) in a generally mildly corrosive environment, with failure occurring below the ultimate tensile strength of the material (Jones, 1992). Once the stress corrosion crack reaches a critical size, which is dependent on both the stress level and the toughness of the material, catastrophic failure of the remaining section occurs.

The safety implications of SCC of rockbolts have been discussed within the industry for several years. SCC of rockbolts has been reported at a significant number of mines both within Australia and globally since the 1990s. Consequently, it is important to understand the different mechanisms behind SCC of rockbolts before an appropriate solution can be developed.

This paper reports a part of the work being undertaken through an ARC Linkage project which is examining the cause of SCC in underground coal mines. Other aspects of the work include full size (Vandermaat et al., 2012a) and coupon (Vandermaat et al., 2012b) testing, both in-situ in mines and within the laboratory environment.

## 2 Failed rockbolts

Sixty eight failed rockbolts from five different mines were obtained for the present study. The rockbolts had failed in a brittle manner, transverse to their axis, as is characteristic of SCC failure of rockbolts (Crosky et al., 2012). An example is shown in Figure 1. Only the section of bolt from the fracture to the threaded end was retrieved in each case, since the remainder of the bolt was still embedded in the rock. The retrieved sections varied from approximately 100–1,500 mm in length. Most of the bolts showed a discernible bend near the location of the fracture when examined along a straight edge. Otherwise, however, the retrieved section was essentially straight, as illustrated in Figure 1. All bolts had a diameter of 22 mm.

Seven of the failed rockbolts, were selected for detailed examination. These were chosen as bolts which showed minimal post-failure corrosion as evidenced by lack of rusting of the overload region of the fracture surface. The bolts were from three different mines, Table 1, and were of four different chemical types, namely:

- 840 Grade – 0.4%C, 1%Si microalloyed steel.
- Low silicon 840 Grade – 0.4%C, 0.35%Si microalloyed steel.
- AISI 1355 – 1.5% manganese steel.
- AISI 5155 – 0.5%C chromium steel.



**Figure 1** Failed rockbolt as received (Rockbolt 2)

**Table 1** Location of the rockbolts examined

Sample ID	Mine Site
1	A
2	B
3	B
4	A
5	B
6	C
7	A

### 3 Experimental procedure

#### 3.1 Chemical and microstructural characterisation

The chemical composition was determined for each of the seven rockbolts using optical emission spectroscopy. The microstructure of each bolt was examined in metallographically polished sections perpendicular to the axis of the rockbolt using optical microscopy. The hardness of each rockbolt was also determined.

#### 3.2 Examination of subcritical cracks

It has been noted in previous work (Crosky et al., 2012, 2004, 2002) that failed rockbolts sometimes contain cracks extending from the surface which had not propagated to sufficient depth to cause fracture. These cracks are referred to here as subcritical cracks. The seven rockbolts were examined for subcritical cracks using magnetic particle inspection (MPI), after first cleaning the surface using a wire brush. Figure 2 shows an example of subcritical cracks revealed by MPI in Rockbolt 2. As found in the previous work, the cracks were located along the sides of the ribs and ran perpendicular to the axis of the rockbolts.

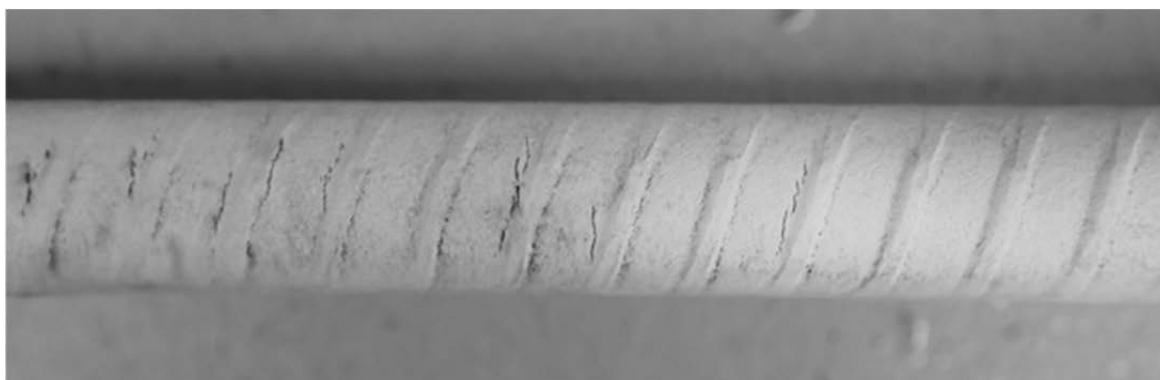


**Figure 2** Subcritical cracking along the ribs of Rockbolt 2 as revealed by magnetic particle inspection

Selected subcritical cracks were sectioned perpendicular to their length and metallographically polished to a 0.25 micron diamond finish. The cracks were examined unetched using optical microscopy. Corrosion product present in the cracks was analysed using a Renishaw inVia laser Raman microscope using 514 nm (green) excitation. Care was taken to avoid heating of the corrosion product during the analysis since this can cause temperature-induced transformation to a different material (Neff et al., 2004).

After the corrosion product had been analysed, the specimens were etched in 5% Nital solution, then examined by optical and scanning electron microscopy (SEM) to establish the relationship between the crack path and the microstructure of the rockbolts. Where necessary, electron backscatter diffraction

(EBSD) was used to determine the grain orientation on either side of the crack to establish whether the crack was running through a single grain or along the boundary between two adjoining grains.

### 3.3 Examination of fracture surface

The fracture surfaces were examined by low power stereo optical microscopy, then at higher magnification using scanning electron microscopy. The stress corrosion region of the fracture surfaces necessarily contained corrosion product and it was necessary to remove this prior to SEM examination. This was done by ultrasonically cleaning the fracture surface in a water/detergent mixture to remove any loose corrosion product. This was followed by ultrasonic cleaning in Ajax inhibited hydrochloric acid for a maximum of 10 seconds.

## 4 Results and discussion

### 4.1 Chemical composition

The chemical composition of the seven rockbolts examined is given in Table 2. As noted earlier, the rockbolts had been manufactured from four different grades of steel, 840 Grade (Rockbolts 1–3 and 6), a low silicon version of 840 grade (Rockbolt 5), AISI1355 (Rockbolt 7) and AISI 5155 (Rockbolt 4).

**Table 2** Composition of the failed rockbolts examined

Sample ID	%C	%Mn	%Si	%Ni	%Cr	%Mo	%S	%P	%Cu	%V	%W	%Ti	%Al
1	0.37	1.49	1.09	0.02	0.03	0.001	0.013	0.021	0.006	0.037	0.023	0.001	0.008
2	0.38	1.55	1.13	0.02	0.03	0.002	0.018	0.024	0.01	0.037	0.019	0.002	0.005
3	0.39	1.49	1.03	0.02	0.03	0.001	0.015	0.024	0.01	0.041	0.019	0.002	0.004
4	0.56	0.81	0.25	0.03	0.76	0.005	0.018	0.029	0.01	0.008	0.023	0.002	0.027
5	0.40	1.44	0.35	0.05	0.06	0.010	0.027	0.015	0.18	0.048	0.020	0.001	0.004
6	0.37	1.55	1.10	0.03	0.02	0.001	0.012	0.014	0.007	0.025	0.018	0.003	0.004
7	0.54	1.65	0.25	0.10	0.09	0.02	0.02	0.013	0.202	0.002	0.016	0.001	0.003

### 4.2 Microstructure

The microstructures of Rockbolt 1 (840 Grade steel) Rockbolt 7 (AISI 1355) and Rockbolt 4 (AISI 5155) are shown in Figure 3. All three rockbolts showed surface decarburisation which had resulted from the hot rolling process used in their manufacture. The 840 Grade steel had a mixed ferrite/pearlite structure. The AISI 1355 steel had a mostly pearlitic structure with just a small amount of ferrite at the prior austenite grain boundaries while the AISI 5155 steel was almost fully pearlitic. The low silicon 840 Grade steel (Rockbolt 5) had a similar microstructure to the 840 Grade steel. All steels contained longitudinal manganese sulphide inclusions (stringers), as is characteristic of air melted steels.

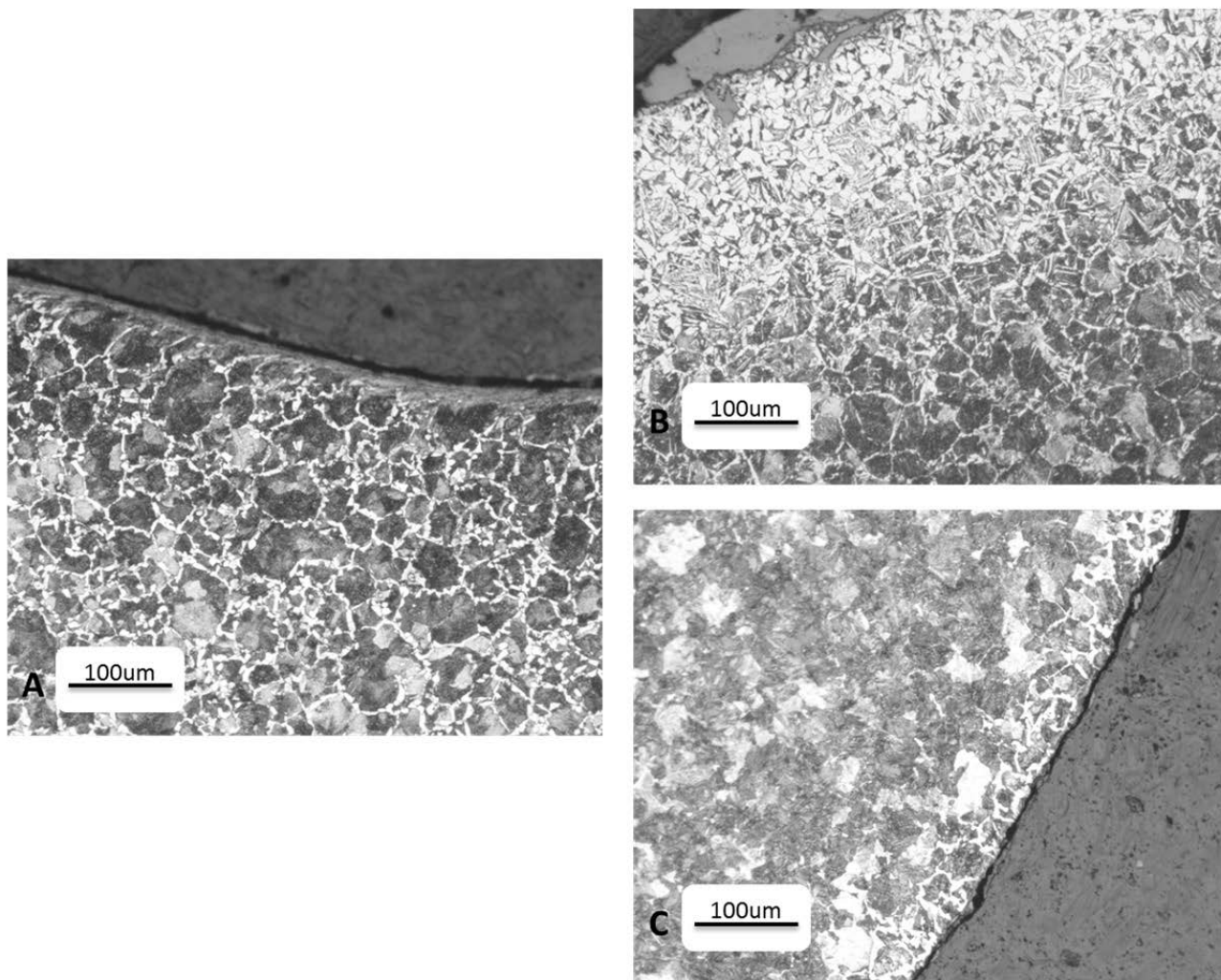


**Figure 3** Microstructure of (A) Rockbolt 1 (840 Grade steel), (B) Rockbolt 7 (AISI 1355 steel) and (C) Rockbolt 4 (AISI 5155 steel)

### 4.3 Hardness

The hardness of the rockbolts examined is given in Table 3. The values given are the average of four readings taken midway between the centre and surface of each rockbolt. The hardness values range from 250–320 HV<sub>30</sub>.

**Table 3** Hardness values of failed rockbolts

Sample ID	Hardness HV <sub>30</sub>
1	313
2	266
3	285
4	321
5	259
6	250
7	316

#### 4.4 Underground mine water analysis

Analyses of the ground water from Mine A (Rockbolts 1, 4 and 7) and mine B (Rockbolts 2, 3 and 5) are given in Table 4. There are significant differences between the two mine waters. Mine B has a higher pH than Mine A (9.11 compared with 7.95). It also contains a much higher concentration of sulphate, carbonate and bicarbonate ions. However, the level of dissolved oxygen was similar for the two mines.

**Table 4** Chemical analysis of mine water from the two different mines

Physico-Chemical Characteristics	Units	Mine A	Mine B
pH	pH units	7.95	9.11
Total dissolved solids	mg/L	618	3,227
Dissolved oxygen	mg/L	7.2	6.67
Sulfate	mg/L	39	81,764
Chloride	mg/L	8	15
Alkalinity (total) as CaCO <sub>3</sub>	mg/L	355	2,882
Carbonate	mg/L	0	199
Bicarbonate	mg/L	355	2,683

#### 4.5 Subcritical cracks

Two quite different types of subcritical crack were observed, as shown in Figure 4. The first were narrow cracks with minimal lateral corrosion of the crack walls Figure 4(a), while the second were broader cracks which had undergone substantial lateral corrosion of the crack walls, Figure 4(b). Only one type of cracking was, however, observed in any given rockbolt.

A similar difference in crack type has been reported for groundwater-induced SCC of pipeline steels (Beavers and Harle, 2001). The first type of crack was observed in high pH (>9) groundwater and has been attributed to bicarbonate cracking. The second type was observed in near neutral (pH of 5–7.5) groundwater and was attributed to a hydrogen induced cracking mechanism (Beavers and Harle, 2001).

The rockbolt shown in Figure 4(a) was from Mine B which had a high pH/high bicarbonate groundwater, whereas the rockbolt shown in Figure 4(b) was from Mine A which had a near neutral pH low bicarbonate groundwater (Table 4). These findings are consistent with the prior findings for pipeline SCC and, accordingly, the two types of crack will hereafter be referred to as high pH and near neutral SCC.

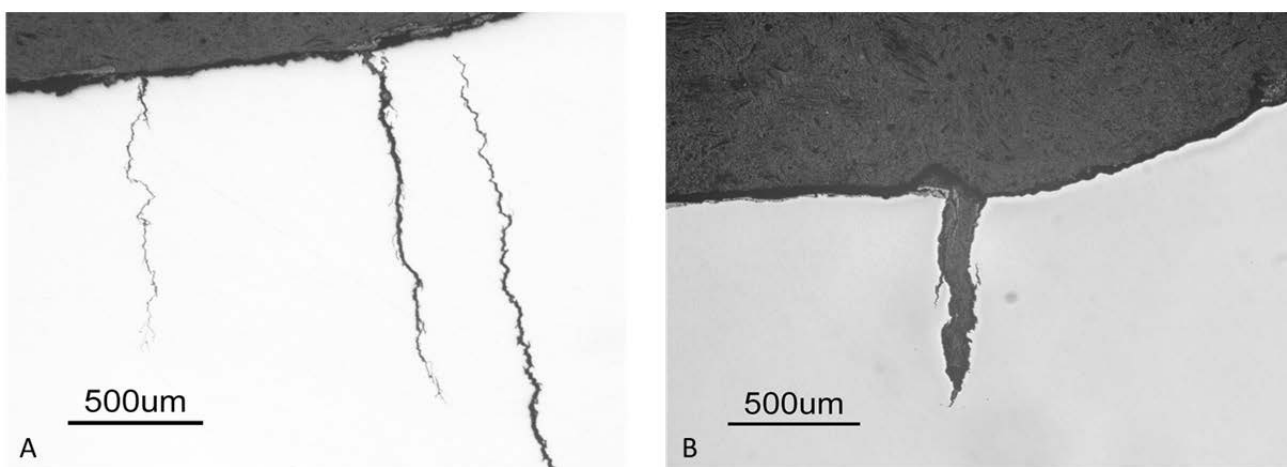


**Figure 4** Subcritical cracks (A) in Rockbolt 5 (B) in Rockbolt 1

Careful examination of the surface of Rockbolt 1 (near neutral environment) revealed that, in the early stages of development, cracks in the rockbolt were often associated with cracks in the mill scale (Figure 5), which remains on the surface from the hot rolling process. It has been reported that mill scale is expected to be a factor in near neutral pH SCC of pipelines (Beavers and Harle, 2001). No association between cracking of the mill scale and the underlying cracks in the rockbolts has been observed to date for the high pH environment in the present study, but mill scale has been reported to contribute to the formation of high pH SCC of pipeline steels (Beavers and Harle, 2001).

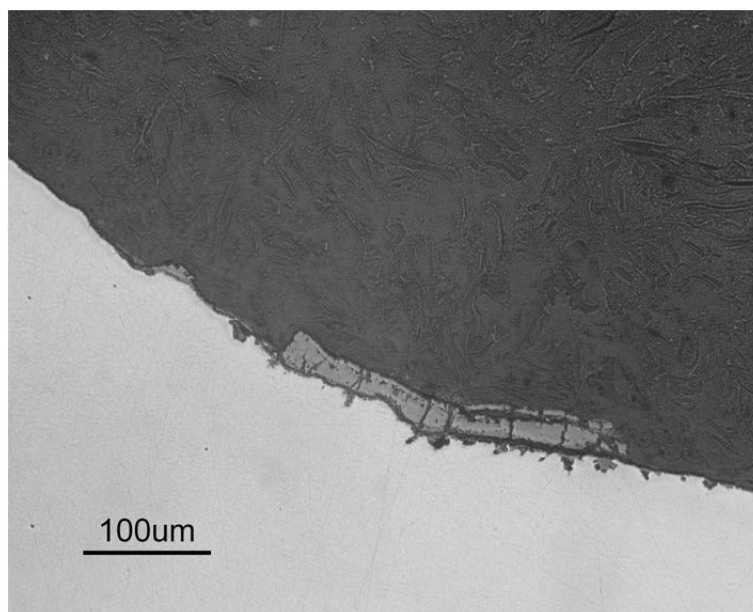


**Figure 5** Cracks in Rockbolt 1 emanating from cracks in mill scale

#### 4.6 Analysis of corrosion product

Analysis of the corrosion product was undertaken using microRaman spectroscopy for the high pH and near neutral cracks. The high pH crack examined (Rockbolt 5) is shown in Figure 6, while the spectrum obtained is shown in Figure 7. Comparison of the spectrum with the Renishaw database indicated that the main component of the corrosion product was  $\text{FeCO}_3$  (siderite), consistent with the proposed carbonate cracking mechanism.

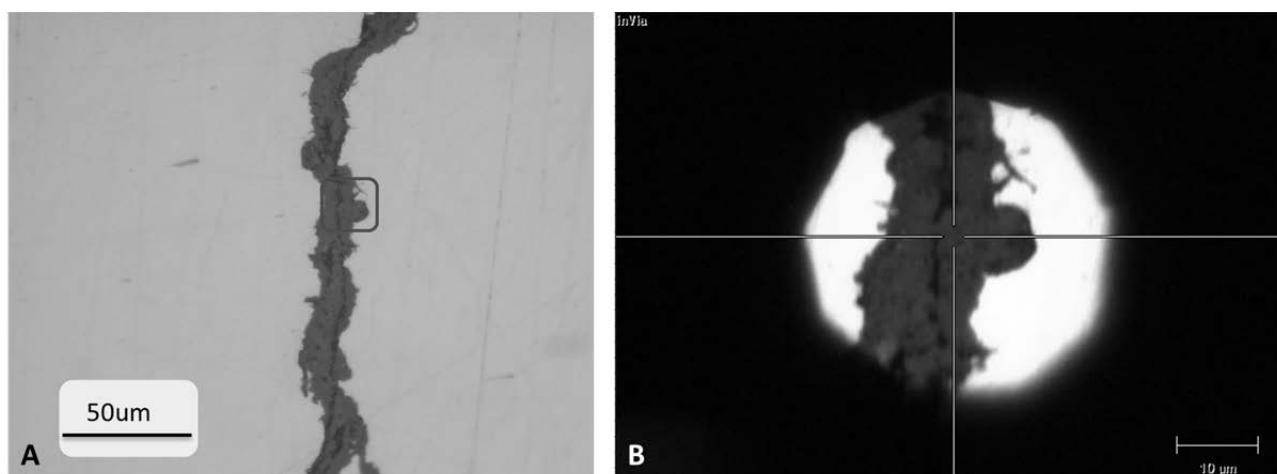


**Figure 6** High pH crack in Rockbolt 5: (A) optical microscope image; (B) raman microscope image of boxed region in (A). Cross hairs in (B) show site of analysis

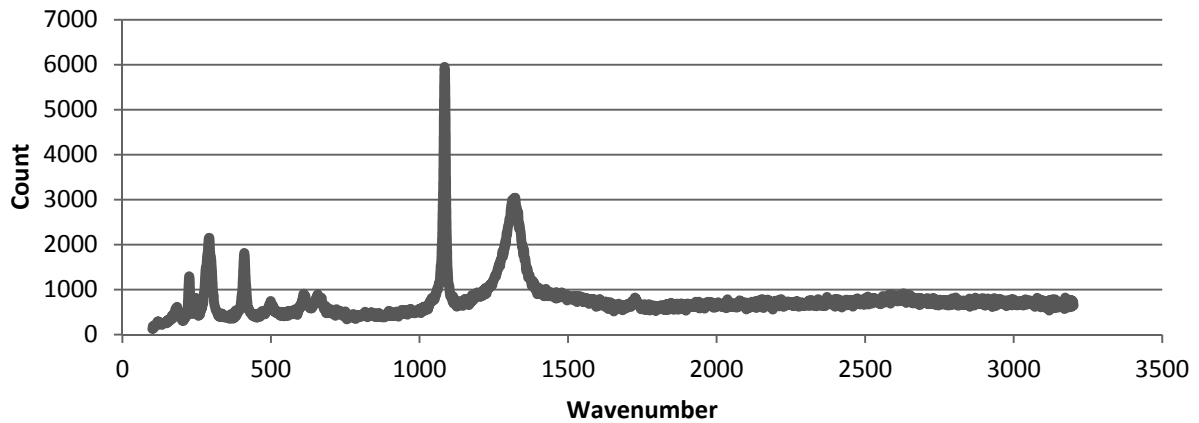


**Figure 7** Raman spectrum of corrosion product in high pH crack shown in Figure 6

The near neutral pH crack (Rockbolt 1) in which the corrosion product was analysed is shown in Figure 8. In this case, analysis of the spectrum, Figure 9, using the Renishaw database indicated that the main component of the corrosion product was  $\text{Fe}_3\text{O}_4$  (magnetite).

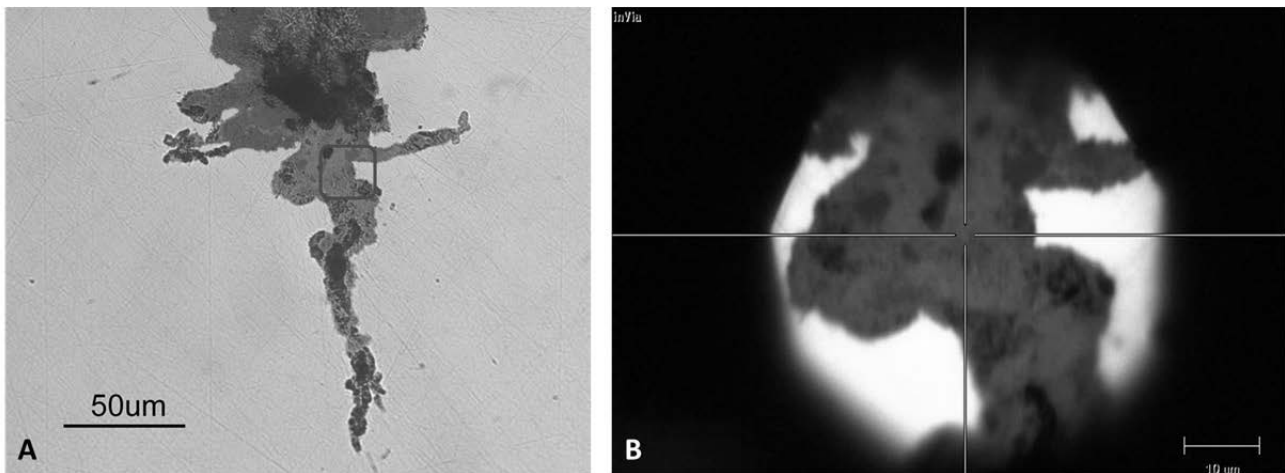


**Figure 8** Near neutral pH crack in Rockbolt 1: (A) optical microscope image; (B) Raman microscope image of boxed region in (A). Cross hairs in (B) show site of analysis

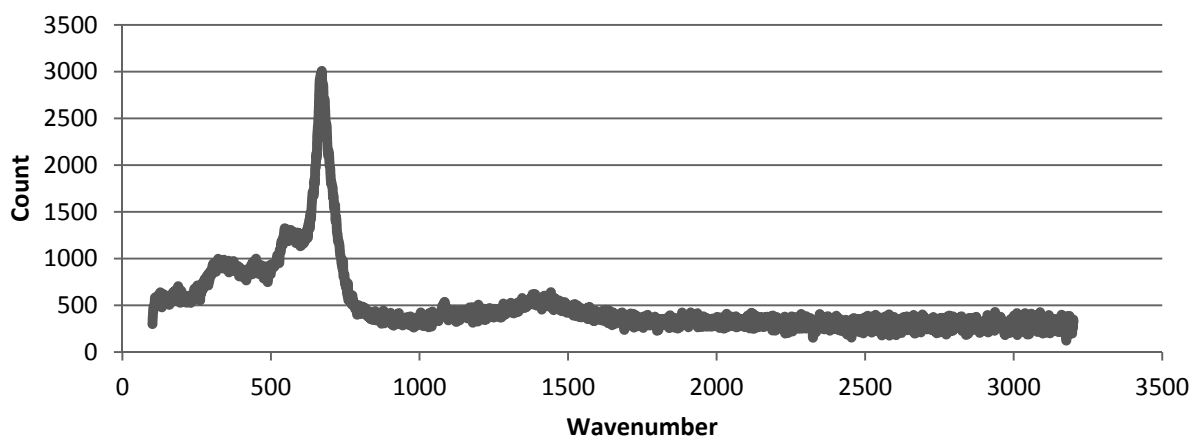


**Figure 9** Raman spectrum of corrosion product in near neutral pH crack shown in Figure 8

#### 4.7 Crack path examination

Optical micrograph of the crack path for a high pH crack (Rockbolt 5) in the low silicon 840 grade steel (ferrite/pearlite structure) is shown in Figure 10. The crack can be seen to run through the pearlite between the individual lamellae (Region A), where the colonies are oriented approximately parallel to the macroscopic crack direction, but between the colonies (Region B), or along the ferrite/pearlite boundaries (Region C), where the pearlite colonies are oriented more perpendicular to the macroscopic crack direction. Similar behaviour has been reported for in-service SCC of X52 pipeline steel (Li et al., 2006).

An SEM micrograph and matching EBSD image of the region of the crack shown in Figure 10c is shown in Figure 11. The crack passes through two adjoining regions of ferrite labelled X and Y in Figure 11(a). EBSD indicated that these two regions have the same orientation Figure 11(b), thus establishing that crack is cutting through a ferrite grain, and not running along the boundary between two adjoining grains.

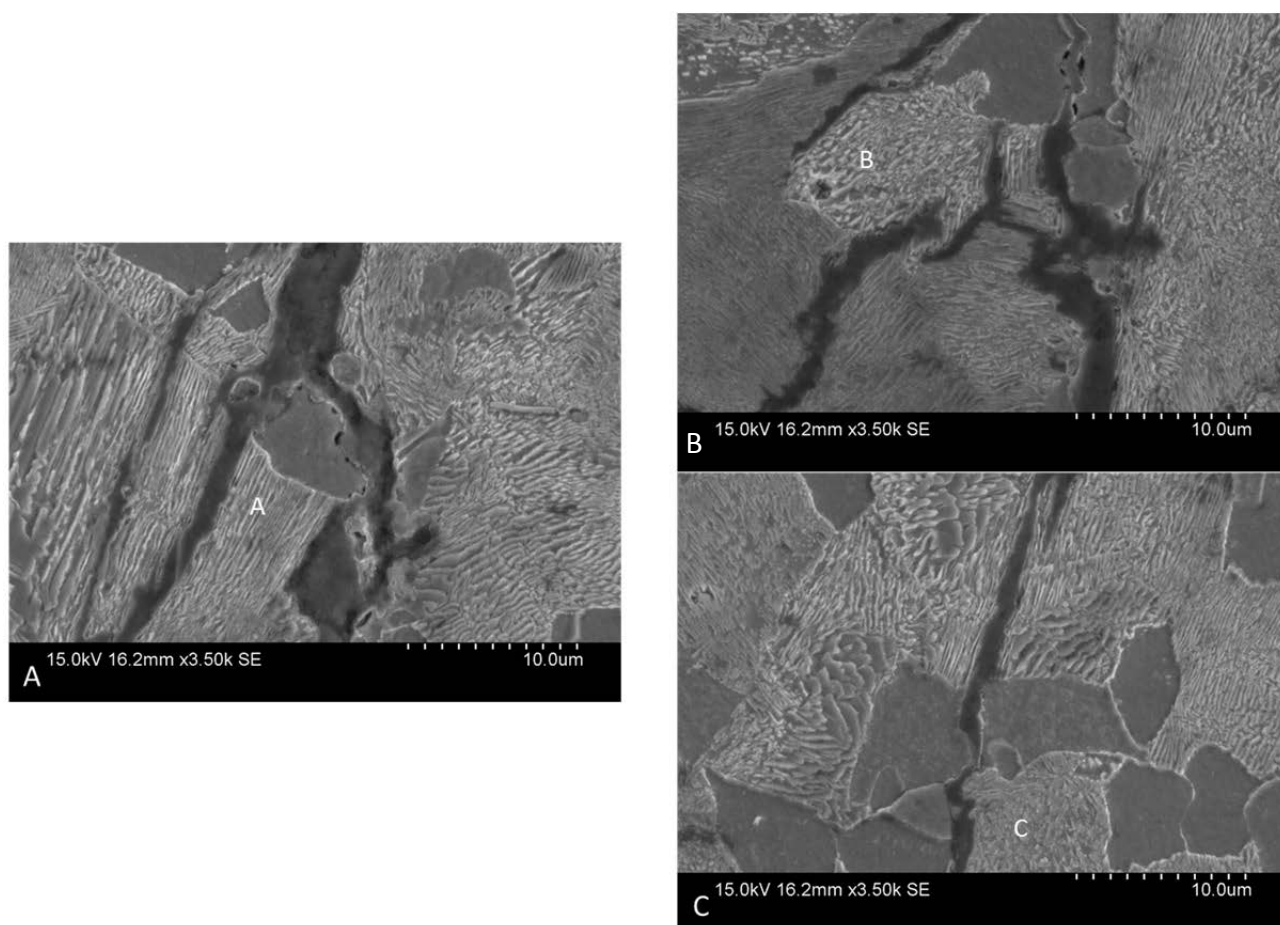


**Figure 10** SEM images showing the crack path for a high pH crack in a low silicon 840 Grade steel rockbolt. The crack runs between the pearlite lamellae in the region marked A, between the pearlite colonies in the region marked B and along the pearlite/ferrite boundary in the region marked C

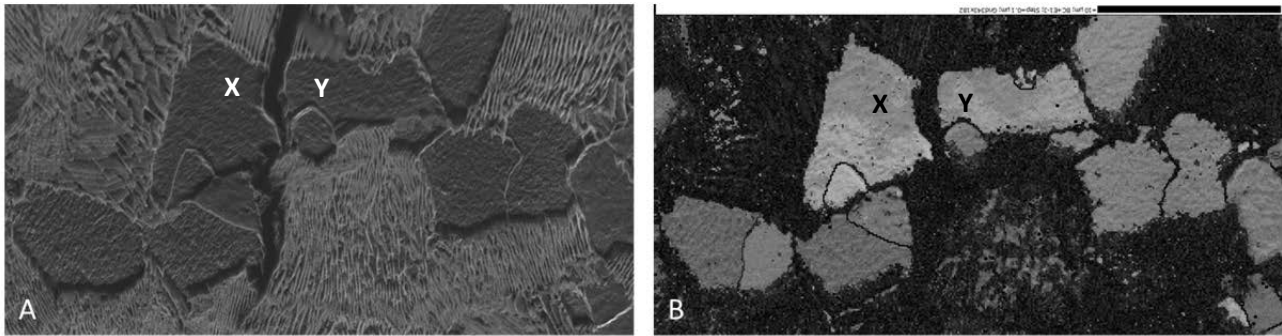


**Figure 11** SEM micrograph and matching EBSD image of crack running through two adjoining regions (marked X and Y) of ferrite

#### 4.8 Examination of fracture surface

An optical fractograph showing the fracture surface of Rockbolt 1 is given in Figure 12. The fracture surface exhibits a thumbnail-shaped discoloured region produced during propagation of the stress corrosion crack, followed by a bright region produced by the final catastrophic overload failure. SEM fractographs of the SCC region and the overload region are shown in Figure 13(a) and (b), respectively. The two regions are distinctly different, with Figure 13(a) showing the features characteristic of SCC while Figure 13(b) shows the features characteristic of brittle overload failure, as reported previously (Crosky et al., 2012; 2004; 2002). It is noted that rockbolts show ductile overload when tested in tension. The brittle overload seen in the SCC failed rockbolts is due to the stress concentrating effect of the notch produced by the sharp stress corrosion crack.



**Figure 12** Optical fractograph of Rockbolt 1

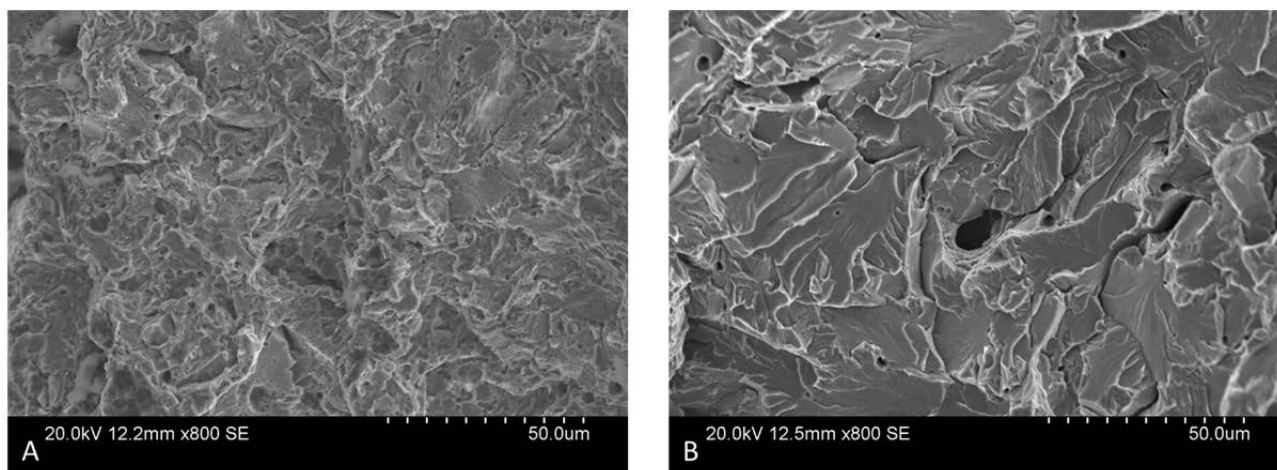


**Figure 13 SEM fractographs of Rockbolt 1 (A) SCC region, (B) overload region**

## 5 Conclusions

The results show that two different types of stress corrosion cracking are occurring in rockbolts in underground coal mines. The first occurs in relatively high pH (>9) environments which are associated with high bicarbonate mine water. The second occurs in near neutral (pH of 5–8) environments with low bicarbonate levels. These findings are consistent with the findings of earlier studies of groundwater-induced SCC of pipeline steels.

## Acknowledgements

Financial assistance from the following organisations and companies is gratefully acknowledged: Australian Research Council (ARC), Australian Coal Association Research Program (ACARP), Jennmar Australia Pty Ltd, Centennial Coal Pty Ltd, Xstrata Coal Pty Ltd, Whitehaven Coal Pty Ltd, and Anglo Coal Australia.

## References

- Beavers, J.A. and Harle, B.A. (2001) Mechanism of High-pH and Near-Neutral-pH SCC of Underground Pipelines, *Journal of Offshore Mechanics and Arctic Engineering*, Vol. 123(3), pp. 147–151.
- Crosky, A., Smith, B., Elias, E., Chen, H., Craig, P., Hagan, P., Vandermaat, D., Saydam, S. and Hebblewhite, B. (2012) Stress corrosion cracking failure of rockbolts in underground mines in Australia, in *Proceedings AIMS 2012 Seventh International Symposium of Rockbolting and Rock Mechanics in Mining*, 30–31 May 2012, Aachen, Germany.
- Crosky, A., Fabjanczyk, M., Gray, P. and Hebblewhite, B. (2004) Premature rock bolt failure Stage 2, ACARP Project No. C12014, final report, Australian Coal Association Research Program, August 2004.
- Crosky, A., Fabjanczyk, M., Gray, P., Hebblewhite, B. and Smith, B. (2002) Premature Rock bolt Failure, ACARP Project No. C8008, final report, Australian Coal Association Research Program, April 2002.
- Gardener, F.J., (1971) History of Rock Bolting, *Symposium on Rock Bolting*, 17–19 February 1971, Wollongong, Australia, Australian Institute of Mining and Metallurgy, Wollongong.
- Jones, R.H. (1992) *Stress-Corrosion Cracking: Materials Performance and Evaluation*, R.H. Jones (ed), ASM International, 445 p.
- Li, J., Elboujdaini, M., Fang, B., Revie, R.W. and Phaneuf, M.W. (2006) Microscopy Study of Intergranular Stress Corrosion Cracking of X-52 Line Pipe Steel, *Corrosion Science*, Vol. 62(4), pp. 316–322.
- Neff, D., Reguer, S., Bellot-Gurlet, L., Dillmann, P. and Bertholon, R. (2004) Structural Characterisation of Corrosion Products on Archaeological Iron – An Integrated Analytical Approach to Establish Corrosion Forms, *Journal of Raman Spectroscopy*, Vol. 35(8–9), pp. 739–745.
- Vandermaat, D., Elias, E., Craig, P., Saydam, S., Crosky, A., Hagan, P. and Hebblewhite, B. (2012a) Experimental Protocol for Stress Corrosion Cracking of Rockbolts, in *Proceedings 12th Coal Operators' Conference*, N. Aziz, B. Kinnimoth (eds), 16–17 February 2012, Wollongong, Australia, Institute of Mining and Metallurgy, pp. 129–136.
- Vandermaat, D., Elias, E., Craig, P., Crosky, A., Hagan, P. and Hebblewhite, B. (2012b) Coupon Testing for Field Assessment of Stress Corrosion Cracking of Rock Bolts, in *Proceedings 31st International Conference on Ground Control in Mining*, T.M. Barczak (eds), 31 July–2 August 2012, Morgantown, USA.

